Vibration Profiles of a Road Ambulance Using Equivalent Acceleration

P. Kehoe[1,4], K. Gibb[1], J. Hurley[1], A. Chan[2], J. Green[2], R. Langlois[1],
K. Greenwood[3], C. Aubertin[3], A. Ibey[2,3] S. Redpath[3],
[1]Department of Mechanical and Aerospace Engineering, Carleton University, Ottawa, Canada
[2]Department of Systems and Computer Engineering, Carleton University, Ottawa, Canada
[3]Children's Hospital of Eastern Ontario, Ottawa, Canada
[4]National Research Council Canada, Ottawa, Canada

Abstract—Neonatal infants in need of advanced care, often require transportation via road ambulance to neonatal intensive care units. The ambulance exposes these vulnerable infants to potentially harmful noise and vibration. To better understand the levels of vibration, this paper maps the magnitude of acceleration due to vibration throughout the cabin of an ambulance. By developing a better understanding of the distribution of the vibration magnitude, decisions can be made to determine the optimal placement of the neonatal patient transport system. Using an inertial measurement unit to measure the translational acceleration and angular rates of the vehicle during on-road testing, the equivalent acceleration at any point in the vehicle can be determined, assuming rigid body motion. It is observed that the distance away from the vehicle's centre of gravity increases the amplitude of acceleration. For a relatively smooth section of road, it appears the placement of the neonatal transport system has minimal impact on the acceleration magnitude. This indicates that the frequency-dependant compliant motion of the transport system, in combination with the placement, likely determines vibration level.

Keywords—**neonatal transport, equivalent acceleration, vibration analysis**

I. INTRODUCTION

Interfacility transportation of neonates by road ambulance may expose newborn infants to vibration and noise inherent to the vehicle and transmitted through the ambulance floor, stretcher, and the Neonatal Patient Transport System (NPTS) [1]. The NPTS serves to secure the patient in the moving vehicle while also providing health monitoring and critical life support equipment while en route to Neonatal Intensive Care Units (NICUs). However, there is evidence that suggests the vibration levels of the vehicle are amplified at some frequencies by the NPTS [2], and there are concerns that the location of the NPTS on the ambulance floor may also contribute to the increased levels of vibration experienced by the infants.

The NPTS we are considering in this paper is standard across the four designated Neonatal Centres in Ontario, Canada [3]; however, the position of the NPTS can vary slightly within the ambulance. This paper looks at two configurations, the more laterally-centred configuration used by The Hospital for Sick Children (SickKids) in Toronto, Fig. 1, and the further offset position used by the Children's Hospital

of Eastern Ontario (CHEO) via the Ottawa Paramedic Service (OPS), Fig. 1.

The objective of this paper is to quantify the equivalent acceleration throughout an ambulance to better understand the impact of the NPTS location on vibration levels for the infants. The mapping of equivalent acceleration is conducted on three orthogonal planes to provide a good indication of how the location of the infant in relation to a fixed point on the vehicle will impact the levels of vibration experienced by the infant. Result tables provide the absolute maximum and RMS equivalent acceleration in three directions relative to the vehicle-fixed coordinate system for selected locations in the ambulance.

The equivalent acceleration combines the instantaneous acceleration of a point on a rigid body with the instantaneous components of the acceleration due to gravity, producing a set of equivalent accelerations that are indicative of the forces acting at that point. In this paper, the calculated kinematic acceleration is compared to measured acceleration at four different floor locations to validate this process. By knowing accelerations at any point in the vehicle, the different mounting location of the NPTS can be optimized for the lowest vibration levels. For this paper, the vibration of a section of provincial highway in Ottawa, Canada is analysed and the results are presented.

Figure 1. CHEO in Ottawa has Power-LOAD rail offset to the driver's side of the ambulance (left), while Toronto's SickKids Hospital uses a more centred rail location (right).

II. METHODOLOGY

A. Test Setup

On-road testing of an ambulance equipped with an NPTS was conducted in July 2021. An ambulance was provided by the OPS that included the Stryker (Kalamazoo, Michigan, USA) Power-LOAD system, model 6390. The ambulance used during the road test was a Demers MX-164 Type III Ambulance with a Ford E-450 chassis. CHEO provided an International-Biomedical (Austin, Texas, USA) Neonatal Patient Transport Systems (NPTS), including a 2.5 kg baby manikin, harness, and Geo-Matrix mattress by Blake Medical (Hamilton, Ontario, Canada). The Automotive and Surface Transportation Research Centre, a division of the National Research Council Canada (NRC-AST), provided instrumentation, data collection, and testing services to support the on-road testing. As part of the overall test setup, a Race Technology (Nottingham, England, UK) Speedbox equipped with an inertial measurement unit (IMU), was located at the lateral and longitudinal (lat/long) centre of gravity (CG) location on the floor of the ambulance. The lat/long CG location was determined using under wheel weight scales, Fig. 2, and applying moment balance equations. During this process, the vehicle was ballasted to replicate the in-service loading for the on-road test with people occupying the two front seats, and three seat locations in the cabin of the vehicle. A mass equivalent dead load version of the NPTS or Dead Load Transport System (DLTS) was also loaded in the vehicle during the weighing. Vertically-oriented uni-axial accelerometers were mounted in the four corners encompassing the open floor location where the NPTS is loaded, Fig. 2. Data collection was conducted on an IMC (Berlin, Germany) CRONOSflex Data Acquisition System (DAS) with the IMU and accelerometers sampled at 2 kHz and filtered at 500 Hz.

Figure 2. Test Setup - CG weighing (top-left), NPTS during road test (top-right), SPEEDBOX (bottom-right), Uni-axial floor accelerometer (bottom-left).

The on-road testing covered different road types including provincial highway, arterial, collectors, major collectors, and a section of gravel road, and was conducted with both the real NPTS and DLTS. For this paper, only the provincial highway data are presented, as it is the primary road type used in interfacility transport. Data processing for calculation of the equivalent acceleration required further filtering of the data signals to provide comparable data. This is especially noticeable when processing the angular velocity into the tangential acceleration which presented significant noise above 15 Hz. The translational acceleration data from the IMU and the uni-axial accelerometers were filtered using a fourth-order, no-phase-shift, low-pass Butterworth filter with a cut-off frequency of 20 Hz while the IMU angular rates used the same filter with a cut-off frequency of 10 Hz. The selection of cut-off frequency was conducted by iterating down in cut-off frequencies until the noise level of the equivalent acceleration signal closely matched the profile of the measured acceleration.

B. Equivalent Acceleration Calculations

The equivalent acceleration calculation begins by determining the kinematic acceleration of a point "P" on a rigid body using a known, or measured acceleration at another point "O".

The relative acceleration of point P with respect to point O is derived starting with the position vector of P with respect to O, $\vec{r}_{P/O}$, and differentiating to determine the velocity $\vec{v}_{P/O}$, and again to find the acceleration $\vec{a}_{P/O}$ [4]. The vehicle fixed coordinate system is such that X is in the longitudinal direction with forward being the positive direction. Y in the positive direction points to the right, while positive Z is vertically down. The origin of the coordinate system coincides with the IMU and is located at point O, see Fig. 4.

Differentiating $\vec{r}_{P/O}$ to determine the velocity,

$$\vec{v}_{P/O} = \frac{\mathrm{d}}{\mathrm{dt}}(\vec{r}_{P/O}) \tag{1}$$

$$\vec{v}_{P/O} = \dot{\vec{r}}_{P/O} + \vec{\omega} \times \vec{r}_{P/O} \tag{2}$$

Differentiating Eq. (2) to determine the acceleration,

$$\vec{a}_{P/O} = \frac{\mathrm{d}}{\mathrm{dt}}(\vec{v}_{P/O}) \tag{3}$$

$$\vec{a}_{P/O} = \ddot{\vec{r}}_{P/O} + \vec{\alpha} \times \vec{r}_{P/O} + 2\vec{\omega} \times \dot{\vec{r}}_{P/O} + \vec{\omega} \times \vec{\omega} \times \vec{r}_{P/O} \tag{4}$$

Since the position vector $\vec{r}_{P/O}$ is a fixed position in the vehicle-fixed coordinate system, the rate change of magnitude of the position and velocity terms, $\dot{r}$ and $\ddot{r}$, are zero and Eq. (4) can be reduced.

$$\vec{a}_{P/O} = \vec{\alpha} \times \vec{r}_{P/O} + \vec{\omega} \times \vec{\omega} \times \vec{r}_{P/O} \tag{5}$$

The kinematic acceleration at point P is therefore:

$$\vec{a}_P = \vec{a}_O + \vec{a}_{P/O} = \vec{a}_O + \vec{\alpha} \times \vec{r}_{P/O} + \vec{\omega} \times \vec{\omega} \times \vec{r}_{P/O} \tag{6}$$

where:

$\vec{a}_P$ is the kinematic acceleration of Point P

$\vec{a}_O$ is the kinematic acceleration of the reference Point O

$\vec{a}_{P/O}$ is the relative acceleration of Point P with respect to O

$\vec{\alpha}$ is the angular acceleration

$\vec{\omega}$ is the angular velocity

The right-hand side of the kinematic acceleration equation can be obtained directly from the IMU for the translational acceleration and the angular acceleration can be computed by numerical differentiation of the angular velocity. Using Newton's difference quotient for numerical differentiation of the data, the Δt was evaluated based on the data sampling rate of 2 kHz, with $\Delta t = 0.0005$ sec.

For the derivation of the equivalent acceleration, a free body diagram, Fig. 3, of the NPTS on the cabin floor is considered [4].
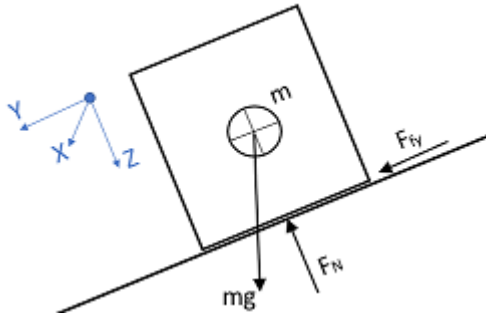

Figure 3. Free-body diagram of NPTS on the ambulance floor.

Applying Newton's second law to the free-body diagram:

$$\sum \vec{F} = m\vec{a} \tag{7}$$

Evaluating both sides of Eq. (7):

$$\begin{Bmatrix} F_{fx} \\ F_{fy} \\ F_N \end{Bmatrix} + [R] \begin{Bmatrix} 0 \\ 0 \\ -mg \end{Bmatrix} = m \begin{Bmatrix} a_x \\ a_y \\ a_z \end{Bmatrix} \tag{8}$$

In Eq. (8), $[R]$ is the rotational transformation matrix that is applied to transform the acceleration due to gravity, g, from the global inertial coordinate system to the vehicle-fixed coordinate system. The mass m can be divided out of the equation, keeping both sides of the equation in terms of acceleration.

$$\frac{1}{m} \begin{Bmatrix} F_{fx} \\ F_{fy} \\ F_N \end{Bmatrix} = [R] \begin{Bmatrix} 0 \\ 0 \\ g \end{Bmatrix} + \begin{Bmatrix} a_x \\ a_y \\ a_z \end{Bmatrix} \tag{9}$$

The resultant equation provides the equivalent acceleration in the X, Y, and Z directions a_{eq_x}, a_{eq_y}, and a_{eq_z}.

$$\begin{Bmatrix} a_{eq_x} \\ a_{eq_y} \\ a_{eq_z} \end{Bmatrix} = [R] \begin{Bmatrix} 0 \\ 0 \\ g \end{Bmatrix} + \begin{Bmatrix} a_x \\ a_y \\ a_z \end{Bmatrix} \tag{10}$$
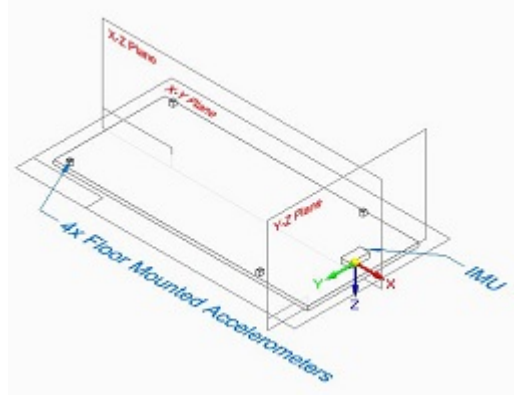

Figure 4. Computer-generated model of the vehicle-fixed coordinate system, ambulance floor, IMU, and floor mounted accelerometers.

Fig. 4 shows the vehicle floor area, the vehicle-fixed co-ordinate system which follows the Society of Automotive Engineers (SAE) standard for wheeled vehicles, the IMU, and four uni-axial accelerometers measuring acceleration at four discrete points on the floor.

C. Validation of Equivalent Acceleration

Validation of the kinematic acceleration computations is conducted by comparing the calculated results to the measured results at the four distinct locations on the ambulance floor where the uni-axial accelerometers were mounted.

A section of road when the ambulance passes over a speed hump at approximately 25 km/hr was used for the comparison. The top plots of the graphs in Fig. 5 and Fig. 6 display the three traces of the IMU data used to determine the equivalent acceleration, while the bottom plots display both the calculated equivalent acceleration and directly-measured acceleration at the discrete locations on the floor. For brevity, only the front left and rear left results are presented here, and demonstrate very similar results to the front right and rear right locations.

These comparisons demonstrate a good match between the measured and the kinematic equivalent acceleration calculated using only the IMU data and validates this approach. This indicates that the mapping of the equivalent acceleration values over the three selected planes and at the selected locations will provide accurate results for rigid body motion.

III. RESULTS

In this paper the equivalent acceleration is evaluated over three planes; the X-Y, X-Z, and Y-Z planes illustrated in Fig. 4. The following contour plots developed in MATLAB use a 150 sec. segment of road data on Provincial Highway 417 between Carling Ave. and Greenbank Road. Plots are provided for each
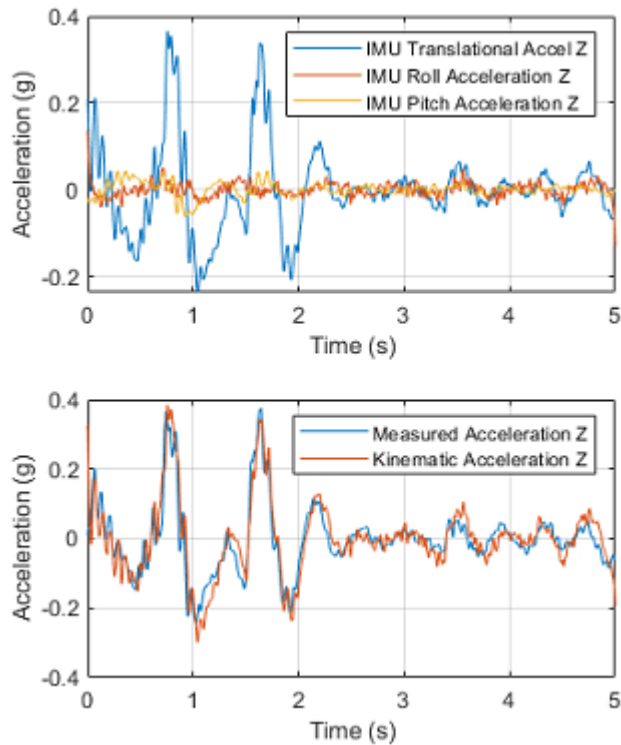
Figure 5. Comparison of the kinematic acceleration to the measured acceleration for the front left floor accelerometer.
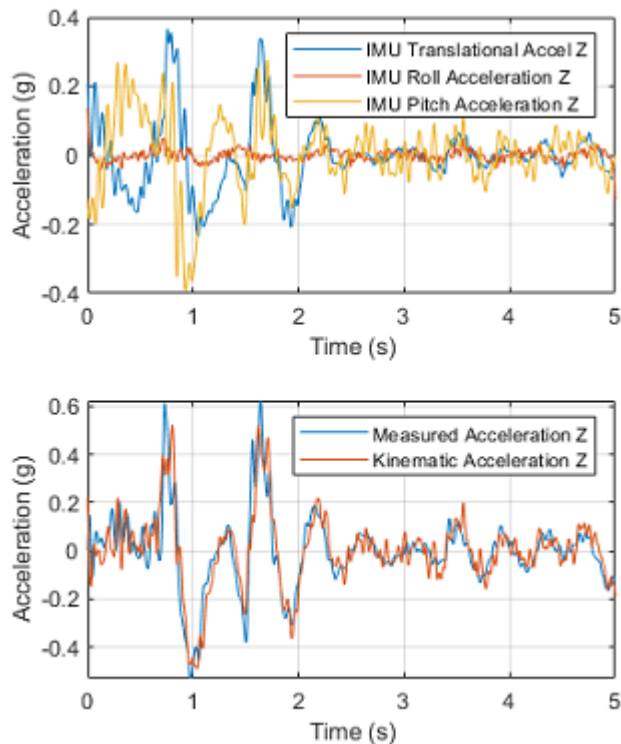

Figure 6. Comparison of the kinematic acceleration to the measured acceleration for the rear left floor accelerometer.

plane showing the Root Mean Square (RMS), Fig. 7, and the absolute maximum equivalent acceleration, Fig. 8. All of the contour plots presented here use a grid pattern with a 10 mm x 10 mm resolution. The side legend provides the magnitude of the acceleration in g's, and the two axes of the plots provide the dimensional information with (0,0,0) being the location of the IMU on the floor. The contribution from gravity was removed as it diluted the overall variation in acceleration.

Table I provides the dimensions for the selected locations that have been evaluated. These locations relate directly to the impact they would have on passengers and the baby assuming all locations are rigidly connected to the ambulance floor. Table II provides the X,Y,Z components of the RMS equivalent accelerations at selected locations in the ambulance. Table III provides the X,Y,Z components of the absolute maximum equivalent accelerations at selected locations in the ambulance.

TABLE I
TABLE OF DIMENSIONS FOR SELECTED LOCATIONS

Location of acceleration	X dir. (m)	Y dir. (m)	Z dir. (m)
Baby's head CHEO	-1.26	-0.22	-0.60
Baby's head SickKids	-1.26	-0.09	-0.60
Driver's seat	1.20	-0.61	-0.36
Front passenger seat	1.20	0.61	-0.36
Captain's seat	0.00	-0.22	-0.44
Fold down seat	0.00	0.53	-0.44
FWD crew bench	-1.01	0.61	-0.44
MID crew bench	-1.52	0.61	-0.44
AFT crew bench	-2.03	0.61	-0.44

TABLE II
TABLE OF RMS ACCELERATIONS BY LOCATION

Location of acceleration	X dir. (g)	Y dir. (g)	Z dir. (g)
Baby's head CHEO	0.036	0.049	0.063
Baby's head SickKids	0.036	0.049	0.063
Driver's seat	0.036	0.048	0.055
Front passenger seat	0.036	0.048	0.057
Captain's seat	0.035	0.047	0.055
Fold down seat	0.036	0.047	0.057
FWD crew bench	0.036	0.048	0.063
MID crew bench	0.036	0.050	0.067
AFT crew bench	0.036	0.052	0.073

TABLE III
TABLE OF ABSOLUTE MAXIMUM ACCELERATIONS BY LOCATION

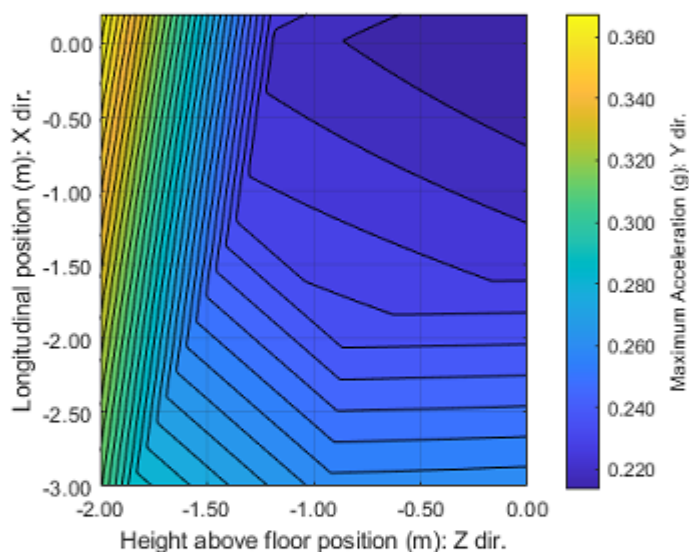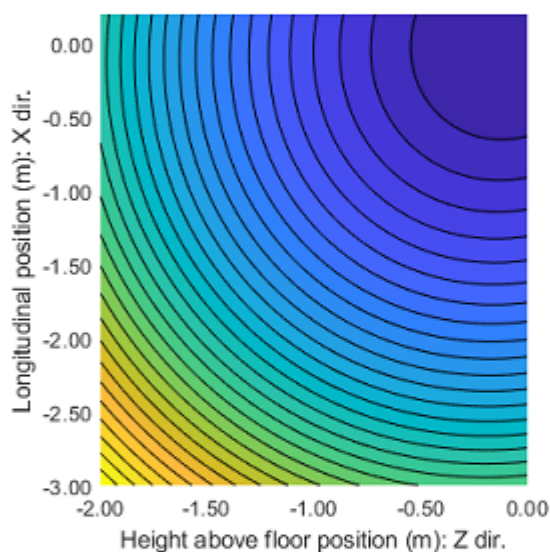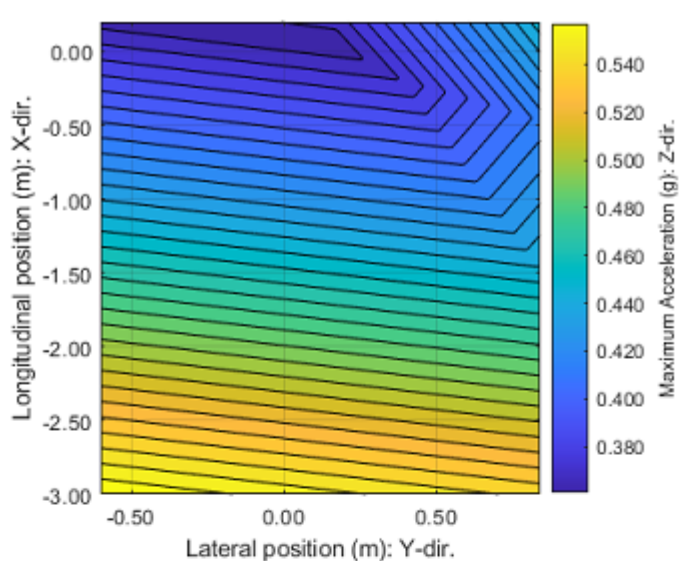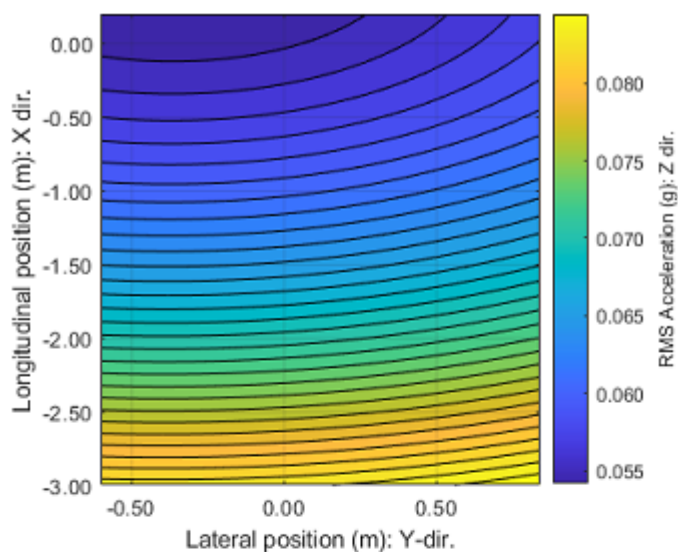| Location of acceleration	X dir. (g)	Y dir. (g)	Z dir. (g)
Baby's head CHEO	0.201	0.228	0.449
Baby's head SickKids	0.202	0.228	0.447
Driver's seat	0.184	0.235	0.424
Front passenger seat	0.195	0.235	0.471
Captain's seat	0.192	0.216	0.371
Fold down seat	0.199	0.216	0.400
FWD crew bench	0.199	0.225	0.421
MID crew bench	0.199	0.230	0.453
AFT crew bench	0.199	0.239	0.485
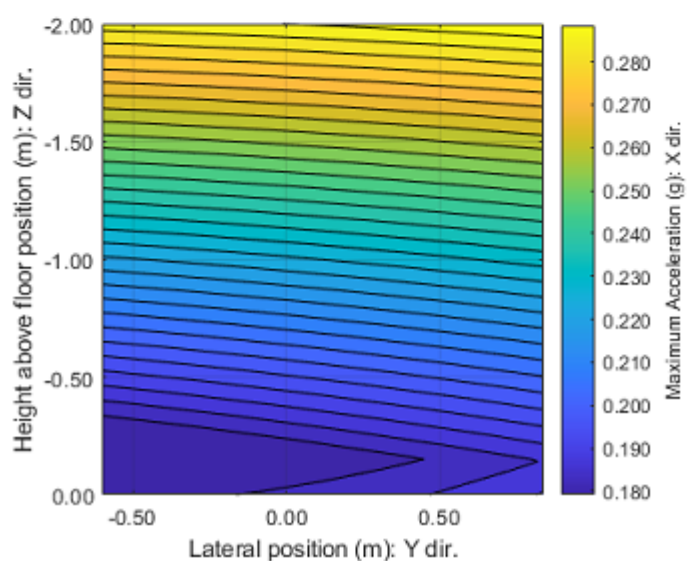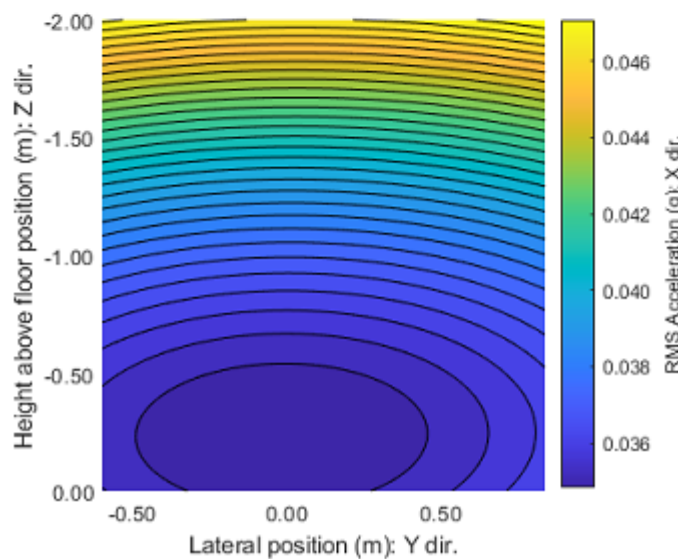
Figure 7. Contour plots for RMS acceleration of a provincial highway for the floor/X-Y plane (top), X-Z plane (middle), and Y-Z plane (bottom).

Figure 8. Contour plots for the absolute maximum acceleration of a provincial highway for the floor/X-Y plane (top), X-Z plane (middle), and Y-Z plane (bottom).

IV. Discussion

This study attempts to quantify the equivalent acceleration of an ambulance floor and two orthogonal planes. In addition, the equivalent acceleration at selected locations that are related to the impact on passengers and the baby are evaluated in all three directions of the vehicle-fixed coordinate system.

The contour plots, Fig. 7 and Fig. 8, provide both the absolute maximum and RMS equivalent acceleration distribution over three orthogonal planes. These accelerations are directed perpendicular to the plane of interest. A more distributed variation in amplitude is observed for the RMS plots than the absolute maximum plots. Both the absolute maximum and RMS plots provide a good indication of how the angular motion of the vehicle affects the magnitude of the equivalent acceleration. With the translational motion effectively constant over the planes, the variation in amplitude is directly related to the angular acceleration multiplied by the relative distance from the reference point for two of the three rotational directions. For example, looking at the floor plane (X-Y) RMS results, top plot of Fig. 7, it is evident that the angular acceleration in pitch of the vehicle amplifies the acceleration as we move away from the IMU towards the back of vehicle. The roll acceleration of the vehicle also contributes to acceleration magnitude, evident by the curved contour lines providing slightly higher amplitude at the sides of the plot. In this example, the yaw motion of the vehicle does not contribute to the floor acceleration in the Z-direction since the yaw motion occurs in plane with the floor.

The contour plots indicate that for the relatively straight and smooth section of provincial highway analyzed, the pitch of the vehicle contributes the most to magnifying the acceleration, followed by roll; and the vehicle is least affected by the yaw motion. In Fig. 7, the plots show that the RMS acceleration varies from 0.055-0.085 g in the Z direction for the floor plane (X-Y), 0.046-0.064 g in the Y direction for the X-Z plane, and 0.035-0.047 g in the X direction for the Y-Z plane.

When looking at the tabulated values of the selected location results we can compare the equivalent accelerations between the more offset NPTS position used by CHEO and the less offset position used by SickKids. The difference between these two mounting positions is 0.13 m in the Y direction. We observe the same results for both CHEO and SickKids in the RMS acceleration for this relatively-smooth section of highway. For the absolute maximum results, the SickKids location presents a slightly higher acceleration in the X direction due to the negative contribution from the yaw motion. The slightly lower value in the Z direction is attributed to the smaller roll contribution during that peak.

The results also indicate that the rear most bench seat location exhibits the highest equivalent accelerations for both the RMS and absolute maximum in the Y and Z directions. This agrees with the results of the contour plots which indicate that the further from the CG of the vehicle, the higher the equivalent accelerations.

V. Conclusions

The determination of equivalent acceleration at any point in the vehicle is possible using a single IMU sensor located at the approximate CG location of the vehicle. It is evident that the further from the CG, the higher the acceleration levels are due to the angular acceleration contributions. The acceleration contour plots presented in this paper can provide an indication of the levels of vibration amplitude of the NPTS if it were firmly fixed to the vehicle floor and the relative motion of the NPTS was eliminated.

The results at the baby's head for the two NPTS mounting locations considered in this paper shows very little difference in amplitude with only slight difference in the X and Z directions of the vehicle-fixed frame of reference for the absolute maximum acceleration. Minimizing the distance from the CG of the vehicle will minimize the vibration magnitude for the infant. Consideration should also be given to the impact on ergonomics for the crew tending to the patient during travel. It should be noted that the road section considered here is a relatively smooth and straight section of road. A rougher road will likely amplify the differences between the CHEO and SickKids mounting positions.

The next steps would be to compare these acceleration values to the accelerations that include the independent motion of the NPTS measured during the road test and to a dynamic model of the NPTS that is being developed [5]. It is believed that the independent motion of the NPTS caused by the compliance in its mounting to the floor causes higher levels of acceleration and quantifying this difference in amplitude will provide insight into possible mitigation techniques. Other road types or high amplitude events can also be analysed to understand how much the location of the NPTS is impacted in those situations.

References

[1] I. Goswami et al., "Whole-body vibration in neonatal transport: a review of current knowledge and fure research challenges", Early Human Development, vol. 146., p. 105051, 01-Jul-2020, doi: 10.1016/j.earlhumdev.2020.1055051.

[2] F. Darwaish et al., "Preliminary Laboratory Vibration Testing of a Complete Neonatal Tranport System," in Proceedings of the Annual International Conference of the IEEE Engineering in Medicine and Biology Society, EMBS, 2020, vol. 2020-July, pp. 6086-6089, doi: 10.1109/EMBC44109.2020.9175852

[3] M. Ramirez et al., "A Provincial Neonatal Transport Incubator for Ontario," in Proceedings of the 37th Conference of the Canadian Medical and Biological Engineering Society (CMBEC37), 2014.

[4] R.G. Langlois, "Determination of Shipboard Equivalent Acceleration", Applied Dynamics Laboratory Report ADL/2004/RGL/1, Carleton University, Canada. May 2004.

[5] K. Gibb et al.,"Developing a Dynamic Model of the Standard Neonatal Patient Transport System using Lagrange's Equation in the Pitch Plane", in Proceedings of the Canadian Society for Mechanical Engineering International Congress 2022